B and N doping in graphene ruled by grain boundary defects

W. H. Brito, R. Kagimura,* and R. H. Miwa
Instituto de Física, Universidade Federal de Uberlândia, CP 593, 38400-902, Uberlândia, MG, Brazil
(Received 1 November 2011; revised manuscript received 12 December 2011; published 3 January 2012)

The energetics and electronic properties of substitutional B (B_C) and N (N_C) doping, and BN codoping in graphene with distinct grain boundary defects were investigated by *ab initio* simulations. Our results indicate that a single B or N impurity atoms and an isolated BN pair prefer to incorporate into the grain boundary region. In particular, we find that the formation of N_C along the grain boundary sites is an exothermic process. It suggests that hexagonal-BN (h-BN) or h-BN and carbon (h-BNC) domains may be patterned by these defective regions. The electronic properties of those doped grain boundary systems have been examined through scanning tunneling microscopy (STM) simulations and electronic band-structure calculations. We find a quite different STM picture for the B_C- and N_C-doped grain boundaries when compared with the same impurities on the perfect graphene sheet.

DOI: 10.1103/PhysRevB.85.035404 PACS number(s): 73.22.−f, 73.22.Pr, 71.55.−i

I. INTRODUCTION

Two-dimensional (2D) materials have attracted wide interest from many researchers in the last few years due to their remarkable physical properties.[1–5] The most promising 2D material is graphene, which behaves as a null-gap semiconductor,[1] whereas hexagonal boron nitride (h-BN), a material with a similar graphenelike structure, exhibits a wide band gap.[2] It is well known that the development of next generations of (nano)electronic devices requires materials with a suitable/tunable electronic band structure. Toward this goal, some approaches using h-BN and graphene have been proposed recently. For example, a very recent experimental work has reported that h-BN domains, immersed in a graphene sheet, open up an energy gap.[4] Also, the authors have shown that the h-BN concentration in graphene can modulate its electronic properties to that required for practical applications.

It is also known that the B and N substitutional doping can modify the electronic properties of carbon nanostructures. Indeed, there are numerous experimental studies addressing the inclusion of impurity atoms in a graphene network, for instance, N-doped graphene sheets upon the presence of NH_3,[6,7] melamine,[8] or N_2 (Ref. 9) molecules. Atomistic simulations, based on *ab initio* methods, have been applied to understand the electronic and structural properties of doped carbon nanostructures,[10,11] while new routes have been proposed for the N and B doping mechanisms in graphene sheets, for instance, the "barrier-free" B doping of graphene[12] and the "controllable healing" of N-doped graphene sheets.[13] Very recently, Åhlgren *et al.* performed a detailed molecular dynamics study of B and N incorporation into graphene layers.[14] The presence of impurity atoms may modify the electronic structure of the doped system, and their presence can be visualized through scanning tunneling microscopy (STM) experiments. Indeed, the modifications on the electronic properties near the B or N (substitutional) sites on graphene have been predicted theoretically[15,16] and verified experimentally.[17,18]

Other carbon nanostructures, like graphene nanoribbons (GNRs), have been considered for B and N doping processes,[19] where theoretical investigations indicate that the impurity substitutional atoms are energetically more stable along the edge sites of the ribbon.[19–22] Edges of GNRs can be considered as an extended topological defect. Extended defects in graphene sheets, such as grain boundary (GB) defects, have been observed in recent experimental investigations.[23,24] Based on *ab initio* simulations and experimental observations,[23–26] structural models for GB defects have been proposed. Also, several calculations suggest that the grain boundary region is very reactive[27,28] and presents a tunable magnetism induced by GB lattice distortion.[29] Indeed, in a recent review, Banhart *et al.* show that the presence of GBs can be useful to tailor in a suitable way the functionality of graphene sheets.[30]

Motivated by those recent experimental and theoretical findings, in this work we have investigated, by means of *ab initio* calculations, the effect of substitutional B and N (BN) (co)doping in the energetics and electronic properties of graphene with grain boundary defects. Our results indicate that the grain boundary region presents the energetically most stable impurity sites for the incorporation of single B or N atoms and the BN pair. This may suggest that the formation of h-BN or h-BN and carbon (h-BNC) domains is more likely to occur at the GB defect than at the graphenelike region. Also, these extended defects could model the h-BN or h-BNC domain shape. Regarding the electronic properties, the incorporation of a single substitutional B (N) dopant atom downshifts (upshifts) the Fermi level, indicating a p-type (n-type) doping in all investigated GB structures. We also performed simulations of STM images for those doped GB structures.

II. COMPUTATIONAL METHOD

Our total energy calculations were performed using the *ab initio* SIESTA code,[31] which is based on the spin-polarized density functional theory (DFT) formalism[32] within the generalized-gradient approximation (GGA).[33] The core states were replaced by norm-conserving pseudopotentials[34] in the factorized form,[35] while the Kohn-Sham orbitals are expressed by a double-ζ plus polarization (DZP) basis set with an energy shift of 100 meV.[36] An energy cutoff of 200 Ry for the real-space mesh was employed. Also, we used 10 (210) special k points in geometry (band-structure) calculations for the Brillouin zone integration.[37] All atomic positions were

fully relaxed until the total forces on each atom were smaller than 10 meV/Å. We have employed the periodic supercell approach and a vacuum space of 15 Å between graphene layers to avoid periodic image interactions. Supercells with (50) 60, 96, and 50 carbon atoms were used to represent the (perfect) defective graphene structures.

III. RESULTS AND DISCUSSION

In order to test our methodology, we begin by calculating the formation energy for the incorporation of substitutional B (B_C) or N (N_C) atoms into a pristine graphene sheet. The formation energy Ω is defined as[38]

$$\Omega = E[X] - E[GS] - \mu_X + \mu_C, \quad (1)$$

where $E[X]$ is the total energy of the supercell containing a substitutional X atom (where X = B or N) into the graphene sheet, $E[GS]$ is the total energy of the pristine graphene sheet, and μ is the atomic chemical potential. In our formation energy (Ω) calculations, we have used the graphene sheet, the N_2 molecule, and the α-boron bulk to obtain the C, N, and B atomic chemical potentials, respectively. We find an Ω value of 1.0 and 0.63 eV/atom for B_C and N_C, respectively. Similar trends are reported in other *ab initio* calculations.[11,21]

Let us now investigate the effect of B and N doping in the energetic properties of GB defects in graphene. The B- and N-doped GB structures are obtained by replacing a single C atom by a B or N impurity, respectively. We have considered, for the GB structures, the structural models used in our previous work[28] and depicted in Fig. 1. Based on their atomic structures, which can be viewed as a suitable regular arrangement of five- and seven- or five- and eight-membered carbon rings along a line in graphene, we have labeled these GB structures as GB1(5-7), GB2(5-7), and GB(5-8). We have considered several B_C and N_C doping sites, as indicated in Fig. 1, in order to find the lowest energy configuration for each GB structure.

The formation energies for the doped grain boundary structures are listed in Table I. From this table, we note that our formation energy results for B_C and N_C incorporated into the graphenelike region (site G in Fig. 1) range from 1.0 to 1.1 eV and 0.4 to 0.5 eV, respectively. These values are in agreement with the ones obtained for the pristine graphene sheet and allow us to infer that the graphenelike regions are described in a suitable way within our (GB) supercell approach. Furthermore, B_C and N_C formation energy calculations indicate that the presence of those impurity atoms along the GB sites is more likely by about 1 eV, in comparison with the pristine graphene sheet. We find formation energies for a substitutional B atom occupying site A ($\Omega[B_A]$) of 0.08, 0.38, and 0.21 eV for GB1(5-7), GB2(5-7), and GB(5-8), respectively, whereas for the graphenelike region we find $\Omega[B_G] \approx 1$ eV. The energetic preference for the GB sites has been strengthened for the N impurity. In this case we obtained $\Omega[N_F]$ of -0.46 and -0.55 eV for GB1(5-7) and GB2(5-7), respectively, while for GB(5-8) we find $\Omega[N_C] = -0.84$ eV. These latter results, i.e., $\Omega[N] < 0$, indicate that the formation of N_C along the (defective) GB sites is an exothermic process. For the lowest energy configurations, we verify that the N atoms occupy the C sites of five- and sixfold rings, giving rise to pyrroliclike structures in GB1(5-7) and GB2(5-7). Meanwhile, B impurities occupy the C sites lying on the six- and sevenfold rings of GB1(5-7) and GB2(5-7). In contrast, due to the peculiar geometry of GB(5-8), the N impurity occupies a C site of five- and eightfold rings, while the B atom lies on a C site shared by the five-, six-, and eightfold rings. The formation of B–C and N–C chemical bonds can be observed in Figs. 2(a)–2(d) and Figs. 2(e)–2(h), respectively. We can infer that the local atomic relaxations rule the energetic preference of those impurities for the GB sites. That is, the covalent radius of B(N) is larger than (similar to) that of C, and comparing the distance between the B (or N) impurity and its nearest C neighbors for the unrelaxed structure, we observe an interesting trend, viz., the B dopant atom prefers the site whose average C–B distance is the largest one, while N prefers the site where the C–N is the smallest one. Moreover, for the relaxed structures, the calculated average B-C (N-C) bond length of 1.55 Å(1.38 Å), 1.52 Å(1.40 Å), and 1.51 Å(1.42 Å) for the most stable GB1(5-7), GB2(5-7), and GB(5-8) structures, respectively, are in agreement with the size of the covalent radius of B and N. In addition, at the equilibrium geometry we observe that the doped GB structures remain planar. It is worth noting that a similar exothermic process has been predicted for N_C along the edge sites of graphene nanoribbons.[21,22]

Now we consider the effect of substitutional doping of B and N on the electronic properties of GB defects. To characterize that, we performed band-structure calculations

TABLE I. Calculated formation energies, in electronvolts, for a single substitutional B and N impurity in grain boundary defects. The letters indicate the doping sites (see Fig. 1).

	GB1(5-7)		GB2(5-7)		GB(5-8)	
	B	N	B	N	B	N
G	1.01	0.52	0.99	0.36	0.98	0.41
A	0.08	0.61	0.38	0.20	0.21	−0.50
B	0.25	0.82	0.40	0.46	0.36	0.19
C	0.61	0.55	0.68	−0.27	0.47	−0.84
D	0.85	−0.14	0.73	−0.17	1.02	−0.67
E	1.47	−0.35	0.79	−0.42		
F	1.53	−0.46	1.56	−0.55		

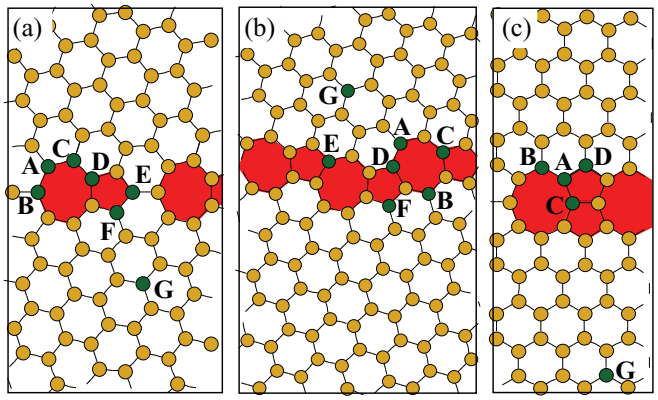

FIG. 1. (Color online) Simulated grain boundary structures, named (a) GB1(5-7), (b) GB2(5-7), and (c) GB(5-8). The doping sites are in green.

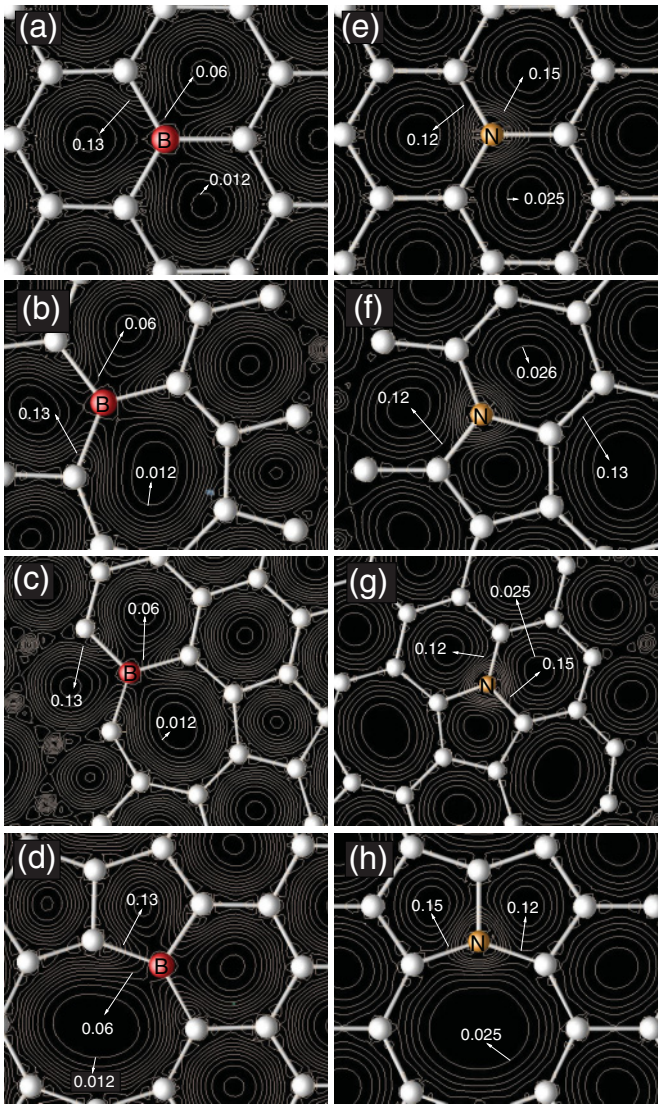

FIG. 2. (Color online) Total charge density for the B_C (left) and N_C (right) atoms in (a) and (e) graphene, (b) and (f) GB1(5-7), (c) and (g) GB2(5-7), and (d) and (h) GB(5-8). The charge densities are in electrons/bohr^3.

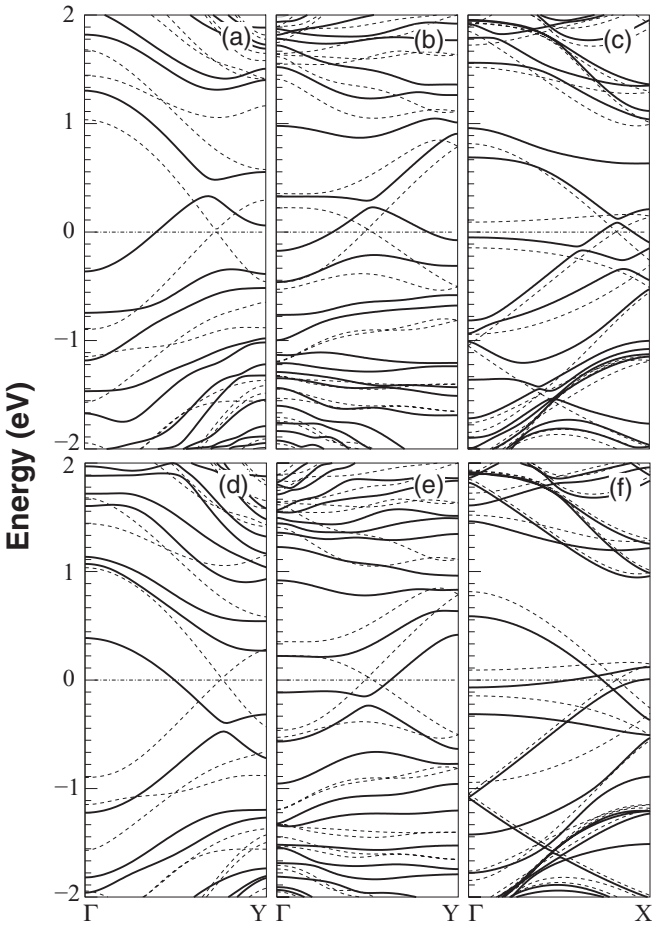

FIG. 3. Electronic band structure for B doped (top panels) and N doped (bottom panels) GB structures. (a) and (d) GB1(5-7), (b) and (e) GB2(5-7), and (c) and (f) GB(5-8). Solid (dashed) lines indicate the band structures for the doped (undoped) systems.

and STM simulations, within the Tersoff-Hamann approach,[39] for the energetically most stable configurations. The electronic band structure for the doped and undoped GB structures is shown in Fig. 3. This figure shows that the basic features of the electronic band structure, near the Fermi level (E_F), of the doped GB structures (solid lines) remain almost the same compared to those of the corresponding undoped ones (dashed lines). However, an interesting trend is observed in their electronic band structures, viz., the incorporation of a single substitutional B atom into the GB defect downshifts the Fermi level, thus indicating a p-type doping, while the N substitutional doping upshifts the Fermi level, in this case indicating an n-type doping for all investigated GB structures. The same behavior has been predicted and observed for B- and N-doped graphene sheets.[7,15,18]

The simulated STM images for the GB structures with B and N substitutional impurities are shown in Fig. 4. Here we have considered energy windows ranging from $E_F - 0.2$ eV (occupied states) and $E_F + 0.2$ eV (empty states) for B and N impurities, respectively. Also, for comparative studies we have simulated STM images for B- and N-doped graphene, depicted in Figs. 4(a) and 4(b), respectively. The STM images (occupied states) of B-doped graphene show a bright (triangular) region centered at the B_C site, spreading out along the B–C bonds. On the other hand, the N_C site becomes darker within $E_F + 0.2$ eV, with bright spots on the C atoms adjacent to the N impurity. In this case we can infer an increase in the electronic density of states (within $E_F + 0.2$ eV) on the C atom's nearby dopant atom. These images are similar to those reported in Refs. 15 and 18.

Figures 4(c) and 4(e) depict the STM images of B-doped GB1(5-7) and GB2(5-7). In the former structure, similar to B_C in pristine graphene, the bright spot lies on the B impurity atom and the nearest-neighbor C atoms, whereas for B_C in GB2(5-7), the bright region is less localized around the B_C site. In contrast, in GB(5-8) [Fig. 4(g)] the B impurity cannot be identified through a bright region; instead, we observe a bright line along the C–C bonds, parallel to the defect line. Such a picture for B_C in GB(5-8) is in agreement with our calculated density of states (not shown) projected onto the B_C atom, which indicates a very small contribution of the

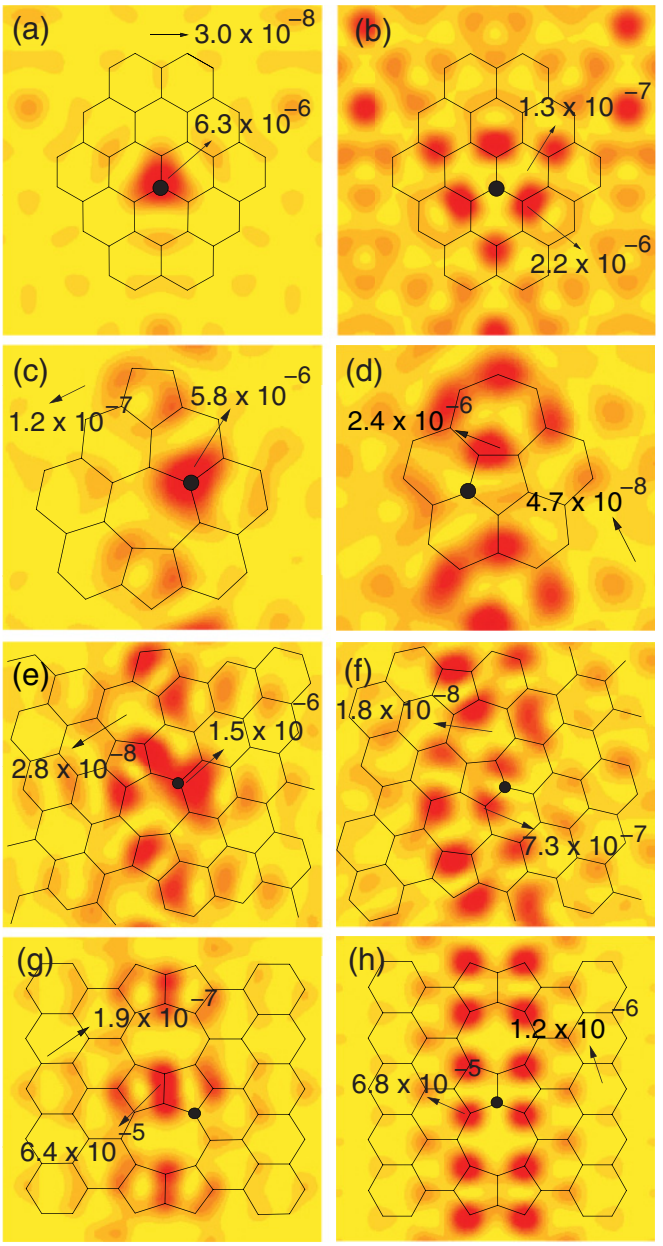

FIG. 4. (Color online) Simulated STM images for B (left panels) and N (right panels) doped: (a) and (b) graphene, (c) and (d) GB1(5-7), (e) and (f) GB1(5-7), and (g) and (h) GB(5-8) structures. An energy window ranging from −0.2 to 0.0 eV and 0.0 to 0.2 eV (relative to the Fermi level energy) was used for the B- and N-doped systems, respectively. The densities are in electrons/bohr^3.

B impurity to the electronic (states) bands near the Fermi level. Our simulated STM images (within $E_F + 0.2$ eV) for N impurities along GB1(5-7) and GB2(5-7) [Figs. 4(d) and 4(f), respectively] show a different picture when compared with N_C in graphene [Fig. 4(b)]. In this case, the increase of brightness is less localized around the impurity atom and does not occur in the same proportion for the nearest-neighbor C atom. In GB1(5-7) there is an increase in brightness of the sevenfold C ring nearest neighbor to the N_C site. In contrast, the increase in brightness upon the presence of N impurity is less evident in GB2(5-7), whereas for the GB(5-8) structure [Fig. 4(h)] the

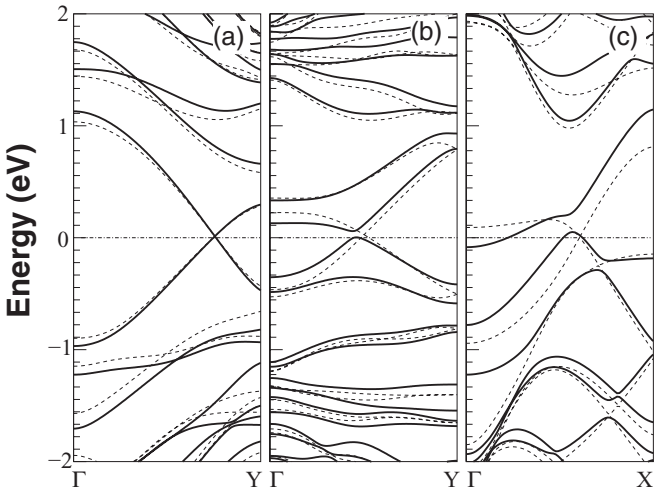

FIG. 5. Our calculated electronic band structures for BN doped (solid line) and undoped (dashed line) (a) GB1(5-7), (b) GB2(5-7), and (c) GB(5-8) structures.

presence of N_C can be detected by the formation of a dark region along the N–C bonds parallel to the GB line.

Since there is an energetic preference for B_C and N_C atoms along the GBs (Table I), it would be interesting to investigate the incorporation of a BN pair into GB structures. To do that we have replaced a single pair of nearest carbon atoms by a BN pair. We have considered several doping sites at the defect region. For the formation energy calculations, we have used ammonia-borane (NH_3-BH_3, the same molecule employed in the synthesis of h-BNC monolayer[4]) and H_2 molecules to calculate the BN pair chemical potential. The

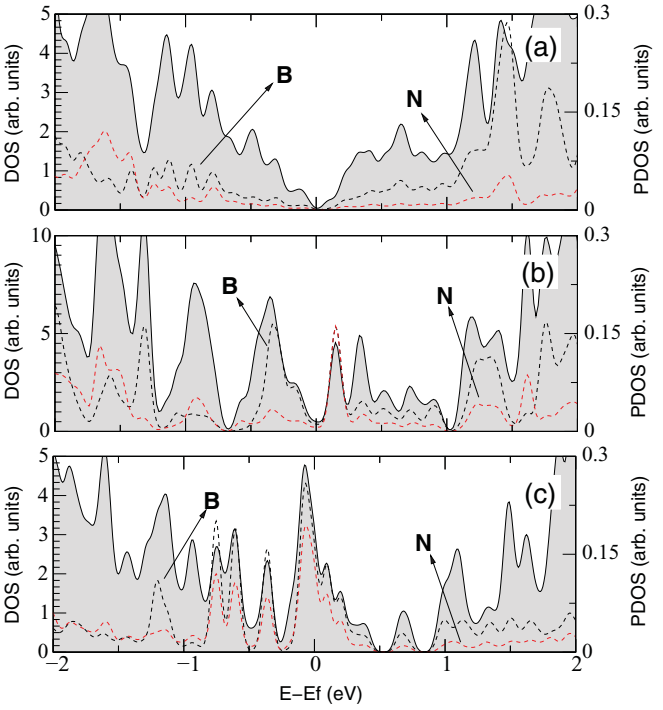

FIG. 6. (Color online) Total (solid line) and projected density of states (dashed line) onto the B and N atoms for the BN codoped (a) GB1(5-7), (b) GB2(5-7), and (c) GB(5-8) systems.

formation energy for the BN pair incorporated into pristine graphene, GB1(5-7), GB2(5-7), and GB(5-8) are 1.42, −0.21, 0.72, and 0.70 eV/pair, respectively, for the most stable sites. In particular, the formation of a BN pair in GB1(5-7) is an exothermic process, while for the other GB systems, the formation energies reduce by ∼0.7 eV (1.4 → 0.7 eV). These results indicate that the substitutional codoping of a BN pair presents lower formation energy at the defect region than in the perfect graphene for all GB structures. It suggests that the formation of h-BN or h-BNC domains in more likely to occur at the GB defect than at the graphenelike region, that is, those h-BN or h-BNC domains can be patterned by the GB structures.

Figure 5 presents the electronic band structure of the BN codoped GBs. Our results, as indicated in Fig. 5(a), show that the band structure of BN codoped GB1(5-7) is pretty similar to that of the corresponding undoped one. Meanwhile the presence of a BN pair in GB2(5-7) and GB(5-8) promotes small modifications relative to that of their corresponding undoped structures. To examine that in more detail, we calculated the projected density of states (PDOSs) onto the BN pair atoms. The PDOS diagrams show that the contribution of the B atom to the total density of states is larger near the conduction and valence band edges for GB2(5-7) and GB(5-8) than for GB1(5-7), as shown in Fig. 6, which is in agreement with their band-structure modifications.

IV. CONCLUSIONS

In summary, we have performed *ab initio* total energy calculations to investigate the effect of substitutional B and N doping and BN codoping in the electronic and structural properties of graphene with grain boundary defects. Our results indicate that the incorporation of N and B atoms into the defective region is an energetically favorable process. In particular, we find that the formation of N_C along the GBs is an exothermic process. Also, the substitutional codoping of the BN pair presents lower formation energy at the defect region than in the perfect graphene for all GB structures. This suggests that the formation of h-BN or h-BNC domains is more likely to occur at the GB defect than at the graphenelike region. The calculated electronic properties show that the incorporation of a single substitutional B (N) atom produces a p-type (n-type) doping in all investigated GB structures. However, the BN codoping introduces only small modifications of their electronic structures.

ACKNOWLEDGMENTS

We acknowledge support from the Brazilian agencies CNPq, FAPEMIG, and CAPES.

*kagimura@infis.ufu.br

[1] K. S. Novoselov, A. K. Geim, S. V. Morozov, D. Jiang, Y. Zhang, S. V. Dubonos, I. V. Grigorieva, and A. A. Firsov, Science **306**, 666 (2004); A. H. Castro-Neto, F. Guinea, N. M. R. Peres, K. S. Novoselov, and A. K. Geim, Rev. Mod. Phys. **81**, 109 (2009), and references therein.

[2] K. S. Novoselov, D. Jiang, F. Schedin, T. J. Booth, V. V. Khotkevich, S. V. Morozov, and A. K. Geim, Proc. Natl. Acad. Sci. USA **102**, 10451 (2005); L. Song, L. Ci, H. Lu, P. B. Sorokin, C. Jin, J. Ni, A. G. Kvashnin, D. G. Kvashnin, J. Lou, B. I. Yakobson, and P. M. Ajayan, Nano Lett. **10**, 3209 (2010).

[3] J. N. Coleman, M. Lotya, A. O'Neill, S. D. Bergin, P. J. King, U. Khan, K. Young, A. Gaucher, S. De, R. J. Smith, I. V. Shvets, S. K. Arora, G. Stanton, H. Kim, K. Lee, G. T. Kim, G. S. Duesberg, T. Hallam, J. J. Boland, J. J. Wang, J. F. Donegan, J. C. Grunlan, G. Moriarty, A. Shmeliov, R. J. Nicholls, J. M. Perkins, E. M. Grieveson, K. Theuwissen, D. W. McComb, P. D. Nellist, and V. Nicolosi, Science **331**, 568 (2011).

[4] L. Ci, L. Song, C. Jin, D. Jariwala, D. Wu, Y. Li, A. Srivastava, Z. F. Wang, K. Storr, L. Balicas, F. Liu, and P. M. Ajayan, Nature Mater. **9**, 430 (2010).

[5] C. Jin, F. Lin, K. Suenaga, and S. Iijima, Phys. Rev. Lett. **102**, 195505 (2009).

[6] B. Guo, Q. Liu, E. Chen, H. Zhu, L. Fang, and J. R. Gong, Nano Lett. **10**, 4975 (2010).

[7] L. S. Panchakarla, K. S. Subrahmanyam, S. K. Saha, A. Govindaraj, H. R. Krishnamurthy, U. V. Waghmare, and C. N. R. Rao, Adv. Mater. **21**, 4726 (2009).

[8] Z.-H. Sheng, L. Shao, J.-J. Chen, W.-J. Bao, F.-B. Wang, and X.-H. Xia, ACS Nano **5**, 4350 (2011).

[9] C. Zhang, L. Fu, N. Liu, M. Liu, Y. Wang, and Z. Liu, Adv. Mater. **23**, 1020 (2011).

[10] J.-Y. Yi and J. Bernholc, Phys. Rev. B **47**, 1708 (1993).

[11] R. Singh and P. Kroll, J. Phys. Condens. Matter **21**, 196002 (2009).

[12] R. B. Pontes, A. Fazzio, and G. M. Dalpian, Phys. Rev. B **79**, 033412 (2009).

[13] B. Wang and S. T. Pantelides, Phys. Rev. B **83**, 245403 (2011).

[14] E. H. Åhlgren, J. Kotakoski, and A. V. Krasheninnikov, Phys. Rev. B **83**, 115424 (2011).

[15] B. Zheng, P. Hermet, and L. Henhard, ACS Nano **4**, 4165 (2010).

[16] R. H. Miwa, T. B. Martins, and A. Fazzio, Nanotechnology **19**, 155708 (2008).

[17] M. Endo, T. Hayashi, S.-H. Hong, T. Enoki, and M. Dresselhaus, J. Appl. Phys. **90**, 5670 (2001).

[18] L. Zhao, R. He, K. T. Rim, T. Schiros, K. S. Kim, H. Zhou, C. Gutiérrez, S. P. Chockalingam, C. J. Arguello, L. Pálová, D. Nordlund, M. S. Hybertsen, D. R. Reichman, T. F. Heinz, P. Kim, A. Pinczuk, G. W. Flynn, and A. N. Pasupathy, Science **333**, 999 (2011).

[19] X. Wang, X. Li, L. Zhang, Y. Yoon, P. K. Weber, H. Wang, J. Guo, and H. Dai, Science **324**, 768 (2009).

[20] T. B. Martins, R. H. Miwa, A. J. R. daSilva, and A. Fazzio, Phys. Rev. Lett. **98**, 196803 (2007).

[21] Y. Li, Z. Zhou, P. Shen, and Z. Chen, ACS Nano **3**, 1952 (2009).

[22] T. B. Martins, A. J. R. Silva, R. H. Miwa, and A. Fazzio, Nano Lett. **8**, 2293 (2008).

[23] P. Y. Huang, C. S. Ruiz-Vargas, A. M. van der Zande, W. S. Whitney, M. P. Levendorf, J. W. Kevek, S. Garg, J. S. Alden, C. J. Hustedt, Y. Zhu, J. Park, P. L. McEuen, and D. A. Muller, Nature (London) **469**, 389 (2011).

[24] J. Lahiri, Y. Lin, P. Bozkurt, I. L. Oleynik, and M. Batzill, Nat. Nanotechnol. **5**, 326 (2010).

[25]O. V. Yazyev and S. G. Louie, Phys. Rev. B **81**, 195420 (2010); Nature Mater. **9**, 806 (2010); J. da Silva Araujo and R. W. Nunes, Phys. Rev. B **81**, 073408 (2010).
[26]P. Simonis, C. Goffaux, P. A. Thiry, L. P. Biro, Ph. Lambin, and V. Meunier, Surf. Sci. **511**, 319 (2002).
[27]S. Malola, H. Häkkinen, and P. Koskinen, Phys. Rev. B **81**, 165447 (2010).
[28]W. H. Brito, R. Kagimura, and R. H. Miwa, Appl. Phys. Lett. **98**, 213107 (2011).
[29]L. Kou, C. Tang, W. Guo, and C. Chen, ACS Nano **5**, 1012 (2011).
[30]F. Banhart, J. Kotakoski, and A. V. Krasheninnikov, ACS Nano **5**, 26 (2011).
[31]J. M. Soler, E. Artacho, J. D. Gale, A. Garcia, J. Junquera, P. Ordejón, and D. Sánchez-Portal, J. Phys. Condens. Matter **14**, 2745 (2002); P. Ordejón, E. Artacho, and J. M. Soler, Phys. Rev. B **53**, R10441 (1996); D. Sánchez-Portal, P. Ordejón, E. Artacho, and J. M. Soler, Int. J. Quantum Chem. **65**, 453 (1997).
[32]W. Kohn and L. J. Sham, Phys. Rev. **140**, A1133 (1965).
[33]J. P. Perdew, K. Burke, and M. Ernzerhof, Phys. Rev. Lett. **77**, 3865 (1996).
[34]N. Troullier and J. L. Martins, Phys. Rev. B **43**, 1993 (1991).
[35]L. Kleinman and D. M. Bylander, Phys. Rev. Lett. **48**, 1425 (1982); X. Gonze, R. Stumpf, and M. Scheffler, Phys. Rev. B **44**, 8503 (1991).
[36]J. Junquera, Ó. Paz, D. Sánchez-Portal, and E. Artacho, Phys. Rev. B **64**, 235111 (2001).
[37]H. J. Monkhorst and J. P. Pack, Phys. Rev. B **13**, 5188 (1976).
[38]G. X. Qian, R. M. Martin, and D. J. Chadi, Phys. Rev. B **38**, 7649 (1988).
[39]J. Tersoff and D. R. Hamann, Phys. Rev. B **31**, 805 (1985).